

THE EFFECT OF SQUARE SPLITTERED AND UNSPLITTERED RODS IN FLAT PLATE HEAT TRANSFER ENHANCEMENT

M. Kahrom*, S. Farievar and A. Haidarie

Department of Mechanical Engineering, Ferdowsi University of Mashhad
Mashhad, Iran

kahrom_m@yahoo.com - said_farivar@yahoo.com

*Corresponding Author

(Received: September 12, 2005 - Accepted in Revised Form: January 18, 2007)

Abstract A square splittered and unsplittered rod is placed in a turbulent boundary layer developed over a flat plate. The effect of the resulting disturbances on the local heat transfer coefficient is then studied. In both cases the square rod modifies the flow structure inside the boundary layer. As a result, a stagnation point, a jet and wake area are generated around the square rod, each making a contribution in disturbing the boundary layer and effect on the heat transfer coefficient from the neighboring flat plate. Effects of distance of square rod from the flat plate, inclusion of a splitter at the downstream of the rod, splitter length and its location relative to the square rod on local heat transfer coefficient in a variety of cases are studied. It is concluded that the effect of stagnation point is always to reduce the local heat transfer; the jet and wake both contribute on increasing heat transfer from the flat plate. The contribution of splitter on disturbing the boundary layer is not significant when compared to the effect of square rod when used alone. Splitter on its own contributes to controlling the wake effect and by changing the wake size and its structure reduces the wake effect on heat transfer. However these all depend on geometrical size and positioning of the splitter.

Keywords Heat Transfer Enhancement, Jet, Splitter, Square Rod, Turbulent Boundary Disturbed, Wake

چکیده لایه مرزی توربولنت روی صفحه تخت توسط یک مقطع مستطیلی تحریک شده است. در نتیجه تحریک توزیع ضریب انتقال حرارت در پائین دست جریان تحت تاثیر قرار می گیرد و در قسمت هائی افزایش و در قسمت های دیگر به صورت نقطه ای کاهش می یابد. سپس یک جدا کننده دو قسمت و یک فوقانی و پائینی پشت مقطع را از یکدیگر جدا می کند و اثر جدا کننده بر تحریک لایه مرزی بررسی می شود. جداکننده در فواصل مختلف در امتداد عمود بر صفحه تخت و در گروه دیگری آزمون در امتداد صفحه تخت و همچنین طول جدا کننده در آزمایشات مختلف تغییر داده می شود و در هر حالت تغییرات نقطه ای ضریب انتقال حرارت و متوسط تحریک ضریب انتقال حرارت با صفحه تخت بدون محرک و با تحریک مقطع مستطیلی مورد مقایسه قرار می گیرند. آزمون با دو نرم افزار مختلف انجام و انطباق نتایج نشان می دهد که وجود جت و یک ایجاد شده توسط تحریک کننده از عوامل افزایش دهنده ضریب انتقال حرارت و نقطه سکون موجب کاهش و جداکننده با توجه به طول و موقعیت قرار گیری در پشت مانع گاه موجب افزایش و گاه موجب کاهش ضریب انتقال حرارت در پائین دست نقطه تحریک هستند.

1. INTRODUCTION

Heat transfer, in many of its applications is limited by the area from which it is to be disposed. Computers, communication and aerospace devices are examples of heat generating sources with such a limitation. In some other applications, such as steam (hot) or cold flow piping, insulation and

reduction of heat transfer it is especially a matter of interest. As a consequence to these demands engineers look for methods controlling heat transfer coefficient locally in forced convection, fluid speed, free stream turbulence intensity is of obvious examples of factors controlling heat transfer coefficient. Both factors directly affect the boundary layer structure and mechanism by which

heat is transferred. While physical viscosity is one of the constant properties being responsible on sub layers thickness and structure, turbulent viscosity in boundary layers is highly affected by turbulence convection from upstream and penetration of free stream turbulence into the boundary layer. In viscous sublayers, the heat transfer is purely controlled by the effect of the viscosity of fluid and sublayer thickness, which is controversially effected by the imposed turbulence from the outer layers.

On the other hand, many experimental reports show that the characteristics of wake, downstream to the bluff bodies can be highly influenced by splitter plates located in the wake area or far downstream to it.

Nakayama et al, [1] placed a splitter attached to the downstream of a cylinder and measured the total drag on the cylinder. As a result, they concluded that the total drag due to the splitter effect was reduced. Tiwary et al [2] applied a steady state computer analysis to the cylinder and splitter attached to the rear stagnation point in a channel flow. Howang et al [3] employed unsteady state analysis for a similar case. Results show that total drag is reduced when a splitter follows the circular cylinder. However, for heat transfer from a cylinder, if the area of the splitter is added as a fin to the total cylinder area, the heat transfer result shows enhancement. But if the cylinder area is counted alone, the heat transfer is reduced. If a splitter is placed at a distance from an obstacle, Nataly and Boisart [4], concluded that the splitter effect on heat transfer and also the Strouhal number of the obstacle is changed. Anderson [5] shows that frequency of the vortex generation is also affected by splitter length. Farhbod and Kahrom [6], (also see references [7,8]) showed that the heat transfer from a flat plate at ZPG is effected locally if a square cylinder is placed near or inside the turbulent boundary layer. A square rod the size of $\delta/D \approx 3$ into the boundary layer and investigated whether the placement of obstacle affects the local heat transfer coefficient. They found that as a result of insertion, a stagnation point, a jet and a wake form around the obstacle and the boundary layer is seriously disturbed. The conclusion was made that the stagnation point was a cause for reduction, while the jet and

wake are causes for increase in the local heat transfer coefficient [6]. In this paper an attempt is made to see how a splitter can change Farahbod's results.

2. MODEL GEOMETRY

In the physical domain the air is assumed as the working fluid, entering parallel to a flat plate at 20°C and speed of 14 m/s. The flat plate is 2 meters long and the square cylinder is placed at a distance at which of $\text{Re}_x \cong 10^6$. The square rod dimensions assumed to be $[D \times D] = [8\text{mm} \times 8\text{mm}]$ or having the relative dimension of $\delta/D \approx 3$, if compared to the boundary layer thickness. The SR is then positioned at variety of distances H_{sq} from the flat plate. The geometries and relevant dimensions are schematically shown in Figure 5.

2.1. Governing Equations and Numerical Method

Two different CFD simulation approaches were used. First TEACH (t) computer code is employed to all the features under consideration. Second, the FLUENT code is used to verify the results. In the first approach in the computational domain, incompressible continuity and momentum equations in the Cartesian coordinate system are solved in the a general form of:

$$\Gamma(q) \equiv \Gamma q \quad (1)$$

If expressed in terms of primitive variables the quantity q is defined as $q = (u, v, p)^T$, then:

$$\Gamma = \begin{bmatrix} Q_v & 0 & \partial_x \\ 0 & Q_v & \partial_y \\ \partial_x & \partial_y & 0 \end{bmatrix} \quad (2)$$

The operator Q_v represents convection and diffusion effects as

$$Q_v = Q - v \Delta \quad (3)$$

Where $Q = u\partial_x + v\partial_y$ and the Laplacian operator is defined as $\Delta = \partial_{xx} + \partial_{yy}$. The energy equation is added to the code in the form of;

$$\rho c_p \left(u \frac{\partial \theta}{\partial x} + v \frac{\partial \theta}{\partial y} \right) = k \left(\frac{\partial^2 \theta}{\partial x^2} + \frac{\partial^2 \theta}{\partial y^2} \right) \quad (4)$$

The boundary layers over the flat plate and that of the square rod surfaces interactively disrupt each other, causing steep changes in flow variables. These disturbances, control boundary layer structure and affect on heat transfer coefficient of the flat plate, are a cause of high shear and large rates of turbulence production in this area. The effected domain includes the viscous dominated region and the strongly inhomogeneous region next to it. As a result, sharp changes of flow variables, including velocity and temperature, occur near the solid surfaces. Variation is highest when closest to the wall and it is very important to capture this near wall variations. In such cases, the conventional method is to arrange fine mesh structures together with the wall function close to the solid surfaces.

Due to simplicity and accurate estimation, in this investigation the law of the wall is accepted to be used up to $y^+ \approx 70$, i.e.:

$$\begin{aligned} u^+ &= y^+, \\ T^+ &= Pr y^+ \\ k^+ &= C_1 y^{+2} \\ \varepsilon^+ &= C_2 \quad \text{if } 0 \leq y^+ < 11 \end{aligned}$$

and

$$\begin{aligned} u^+ &= \frac{1}{\kappa} \ln y^+ + C^+ \\ T^+ &= \frac{1}{\kappa_T} \ln y^+ + B_T \\ k^+ &= \frac{1}{\sqrt{C_\mu}} \\ \varepsilon^+ &= \frac{v}{u_\tau \kappa y} \quad \text{if } 11 \leq y^+ \leq 70 \end{aligned} \quad (5)$$

All constants and normalized variables $()^+$ are defined in the nomenclature. The standard $k - \varepsilon$ model is used in the region away from the wall, where $y^+ > 70$. This model is reported to give

adequate performance for flows around bluff bodies [7,8]. The equation for k , including pressure diffusion terms by a gradient transport model is

$$\partial_t k + U_j \partial_j k = P - \varepsilon + \partial_j ((v + v_T) \partial_j k). \quad (6)$$

It is common to add a parameter σ_k as a denominator for v_T , but the recommended value for this parameter is $\sigma_k = 1$, [9].

In Equation 6

$$P \equiv -\overline{u_i u_j} \partial_j U_i$$

The transport equation for ε essentially has a consistent analogy to k Equation 6:

$$\partial_t \varepsilon + U_j \partial_j \varepsilon = \frac{C_\varepsilon 1^P - C_\varepsilon 2 \varepsilon}{T} + \partial_j \left((v + \frac{v_T}{\sigma_\varepsilon}) \partial_j \varepsilon \right). \quad (7)$$

In both equations for v_T the eddy viscosity model is used

$$v_T = C_\mu k^2 / \varepsilon$$

In Equation 7, T is the turbulent time scale and is defined as $T = K / \varepsilon$, to maintain consistency between the k and ε equations.

Equation 6 is the standard form of turbulence energy, if used as a basis; then dissipation equation dimensionally maps to it, if constants are defined as [10]:

$$\begin{array}{ccccc} C_\mu & \sigma_k & \sigma_\varepsilon & C_{1\varepsilon} & C_{2\varepsilon} \\ 0.09 & 1.0 & 1.3 & 1.44 & 1.92 \end{array}$$

2.2. Boundary Conditions For all solid surfaces of SR, splitter and flat plate, no slip condition have been used. The temperature on SR and splitter surfaces is taken as T_∞ and over the hot flat plate is assumed to be $T_w = 70^\circ\text{C}$. Zero gradients for all variables on the free edges of the flow field has been used, i.e.

$$\frac{\partial u}{\partial y} = 0, v = 0 \text{ and } T = T_\infty.$$

At the inlet boundary, $T = T_{\infty} = 20^{\circ}\text{C}$ and the velocity of air are assumed to be $U_{\infty} = 14\text{m/s}$ while at the outlet boundary the pressure is assumed constant and the pressure and temperature gradient is specified to be $\frac{\partial p}{\partial y} = 0, \frac{\partial T}{\partial y} = 0$. The mass flux

through the outlet boundary is found by means of a convective outflow condition, according to Orlanski [11]. This boundary condition uses an upwind form of the following equation for each velocity component and temperature is:

$$\frac{\partial \phi}{\partial t} + U \frac{\partial \phi}{\partial x} = 0 \quad (8)$$

U is the convection velocity by which property ϕ propagates. For steady state problems, Equation 8 takes the form of:

$$\frac{\partial \phi}{\partial x} = 0 \quad (\text{Where } \phi \text{ represents } u, v, w \text{ or } T)$$

$$P = P_{\infty}$$

2.3. Grid Generation and Code Verification

The Physical domain involves a 2m long flat plate and a very small sized square rod, being 8mm on each side, is placed close to a thin turbulent boundary layer. For the mesh generation in such a complex geometry one has to make decisions consistent to the boundary size and flow field gradients. The accuracy inside a turbulent boundary layer is very much restricted by the number of grids being laid inside the laminar sublayer. There are also limitations on the cell aspect ratio where meshes are grown up towards the free stream. Another factor is the computer execution time and storage. These all make grid generation a difficult task. Starting from the sublayer outwards, the minimum number of grids is limited to be one on the solid wall, and one at $y^+ = 1$, which has to be nearly at $y = 0.0001\text{m}$, ending with at least total of 4 grid points in the sublayer. Assuming the same distribution around the square rod surfaces and keeping the mesh aspect ratio in the range between $1.08 \leq S \leq 1.15$, brings the total number of grids in the computational domain to about:

$$[x \text{ direction grids} \times y \text{ direction grids}] = [400 \times 132]$$

However, dependency of the numerical scheme

on the mesh structure is a serious task to be taken under into consideration. Numerical examination shows that the final solution is highly dependent on the mesh size and stretching of grid spacing. Figure 1 shows the overall accuracy of present program in predicting local heat transfer coefficient of a flat plate when using 400×132 meshes by stretching the ratio of $S = 1.08$. In Figure 2, a comparison is made between solutions for grids by an expansion ratio of $S = 1.08, 1.12$ and 1.15 ; namely cases 1, 2 and 3 as shown in the figure. Since our numerical test is taking place at $Re_x \cong 10^6$ which $x = 1.4 \text{ m}$ from leading edge, the finest meshing is performed at this point. The figure shows that for each value of S , as mesh sizing increases; the solution deviates from experimental values. Another verification test is made on estimation of downstream reattachment length after a back step, Figures 3 and 4. This test was assigned as a benchmark for the validity test of a turbulent scheme in the Stanford conference [12]. Figure 3 shows formation and wide of recirculation zone. In Figure 4 variation of skin friction from a point just at the step, downward to the reattachment point is plotted. The figure shows that as meshing becomes finer, the results in predicting the reattachment point is more closer to experimental results. However, for courser meshing skin friction increases abnormally after completion of reattachment, Figure 4, and deviates significantly from experimental results. One can conclude that these verification tests show that the general trend of numerical solution follows the experimental results and by decreasing the stretching ratio, the solution error reduces significantly.

As discussed before, by assuming 4 grids close to each solid boundary in the laminar sublayer, and expanding grid spacing outwards by S , total grids in the domain results in:

- If $S = 1.08$ total grids in the domain $[x \times y]$ = $[400 \times 132]$
- If $S = 1.12$ total grids in the domain $[x \times y]$ = $[352 \times 112]$
- If $S = 1.15$ total grids in the domain $[x \times y]$ = $[308 \times 98]$

Finer grid settings although very time consuming for present work; do not end up with a much better

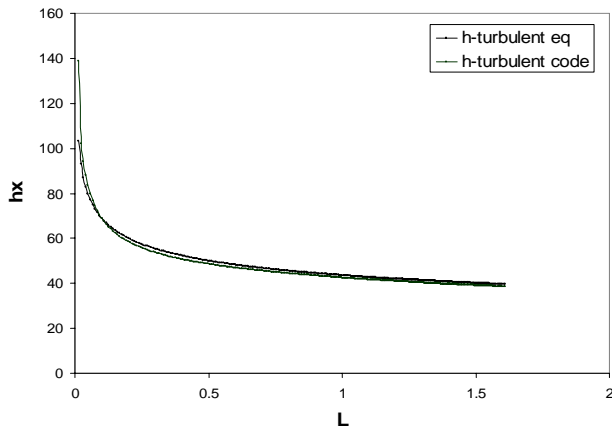


Figure 1. A comparison between solution of present code and experimental results for turbulent flow developing over a flat plate.

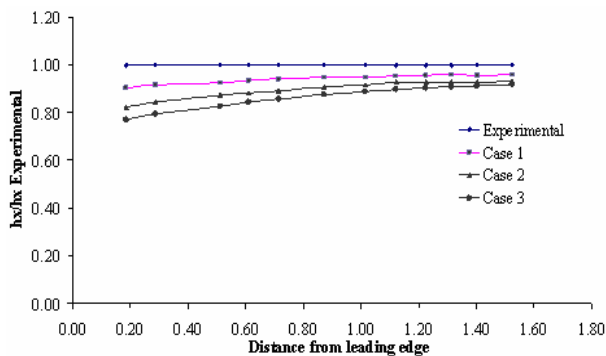


Figure 2. Non - Dimensionalized solution of present program compared to experimental results. Finest meshing is at $x = 1.4$ m from leading edge, then expanding away to both sides. Case 1, 2 and 3 as are defined in the text.

solution than generated for case 1. Thus the stretching ratio of $S = 1.08$ is employed throughout the present work. A typical mesh configuration is presented in Figure 6.

By this assumption, in the case of a single flat plate, the heat transfer coefficient in the laminar portion of the boundary layer was in % 4.6 error and turbulent part was in % 4.2 error with experimental data. In the case of backward facing step, good agreement with standard test data was reached. Present code estimates the reattachment length to be $7.75H$ downstream to step, Figure 3 and 4, where H is the step height. In some references, i.e. [13,9] the reattachment length for turbulent boundary layers is suggested to be

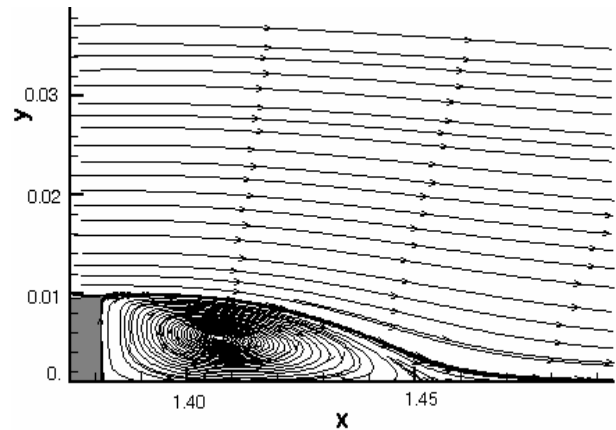


Figure 3. Downstream flow to a back step. Finest meshing is at $x = 1.4$ m. Stretching is made to both sides in x direction and away from the wall in y direction.

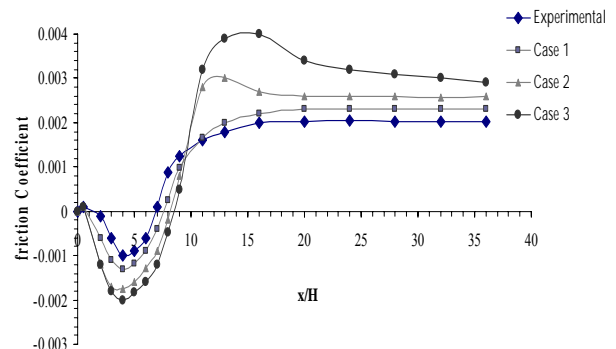


Figure 4. Comparison of skin friction between solutions of present program and experimental results. Cases 1, 2 and 3 are described in the text.

$6.5-7.5H$ which shows the present program overestimating the reattachment length by about % 3.3. The conclusion is made that the present program has reliable accuracy in predicting flow in a disturbed turbulent boundary layer.

In this study, grids are taken to be very fine near the flat plate, around the square rod and the splitter plate. But away from the solid walls where the variables change very smoothly, grids are arranged coarser. Since various positions of the square rod and splitter are to be considered, the total number of grids had to be changed in y direction for each numerical examination. But the general idea in the regeneration of grids remains unchanged throughout the present work.

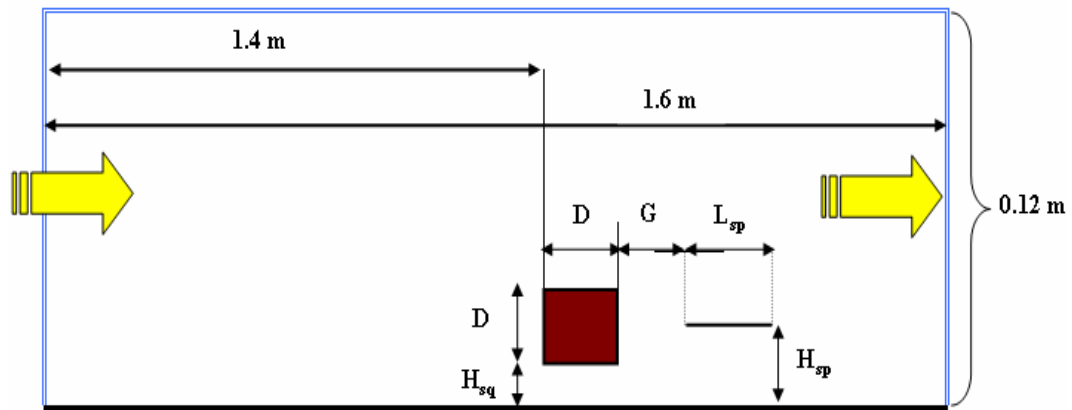


Figure 5. Geometrical consideration of a turbulent boundary layer disturbed by a square rod.

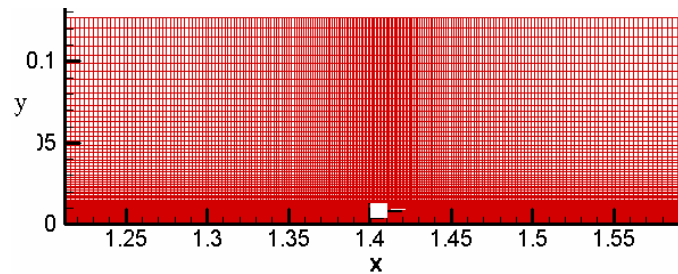


Figure 6. Meshing configuration.

3. RESULTS AND DISCUSSION

This research attempts to invoke the idea that the heat transfer coefficient can be enhanced by imposing a square rod into a turbulent boundary layer. Figure 7 shows that how a stagnation point on frontal area, a jet flow beneath the SR and a wake due to the upper portion of the flow separation form. Unlike flows around a circular cylinder, due to the existence of sharp corners around a square rod, separation points are fixed at rear corners. However, periodic nature of vortex shedding remains unchanged. These all impose disturbances into the neighboring boundary layer over the flat plate. To study such a transient effect, the local heat transfer coefficient at some distinct points of a, b, c, d, e and f, Figure 7, are

presented in Figure 8. In the case of a single square rod without a splitter, three separate flow zones are distinguishable which are a stagnation point on the frontal area which is a serious cause of damping the flow velocity (point b); a jet zone established due to pressure differences on two sides of the square rod causing a sharp increase in local heat transfer (point c) and finally; another increase on heat transfer due to formation of a wide length of wake effect on the rear side at points d and e. Both jet and wake are causes of heat transfer enhancement from the neighboring flat plate. In some locations the heat transfer coefficient is raised by more than 2.5 times of that of a single flat plate at the same Reynolds number. At stagnation point, a reduction of about % 5 in the heat transfer coefficient is observed.

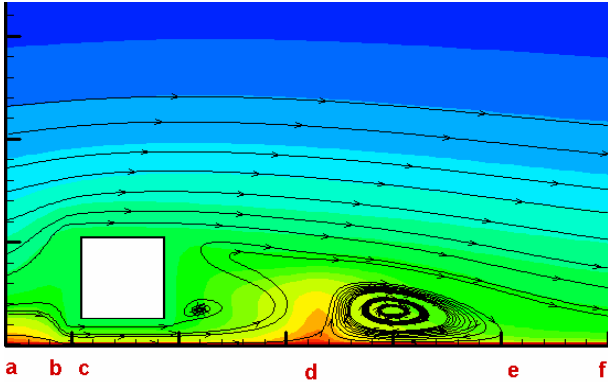


Figure 7. A square rod inside turbulent boundary layer. Position of stagnation point, jet and wake are shown by stream lines.

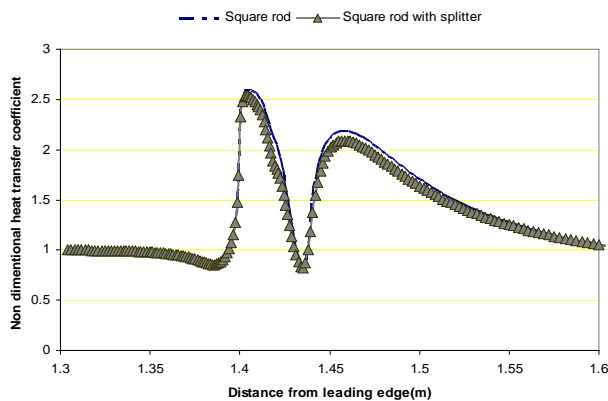


Figure 8. Effect of a single square rod in heat transfer enhancement, (by Farahbod). Local heat transfer coefficient is non - dimensionalized by dividing it with that of a flat plate.

Placing a splitter downstream to SR is expected to control the wake dimensions and reduce interaction between top and bottom wake. As a result, the wake size is expected to affect the formation of jet and stagnation points.

A splitter plate, $L = L_{sp}$, is placed normal to the rear face at a distance of G from the SR and at a distance H_{sp} from the flat plate. All parameters H_{sq} , G , L_{sp} and H_{sp} are factors expected to affect the local heat transfer coefficient. Numerical investigation is conducted to examine the effect of these factors on local heat transfer.

The positioning of SR at distances of $H_{sq} = \{2,4,8,16\}$ mm from the flat plat and the splitter

at a distance from the rod of $H_{sq} = \{2,4,6,8\}$ and assuming the splitter length $L_{sq} = \{2,4,6,8\}$ are all anticipated to contribute in disturbing the boundary layer.

Reference points for investigation are again assigned as a, b, c, d, e, and f, Figure 7. Figure 8 shows relevant local non dimensional heat transfer coefficient at these points which are assigned on Figure7. Point b is exactly at the stagnation point, point c at the beginning of the jet. First, the jet washes away the boundary layer causing a jump in heat transfer coefficient from b to c. Secondly as the jet extends downstream, the heat transfer coefficient falls effectively to point d at which the boundary flow comes to rest and forms another stagnant point. From point e to f a near wall wake enhances the heat transfer again. As an average over all details of flow activity after SR, the local heat transfer coefficient increases over 250 % in some places around the SR. On average about 60 % of the affected area which is assigned as ($L_{\text{effected area}} = 28D$), is placed between points ($x = 1.38$ to 1.67 m) over the flat plate.

In Figure 9, a splitter is placed at the middle of the rear face of the square rod. The splitter length is then changed in steps as $L_{sp} = [0.25,0.5,0.75,1.0] D$. The effect on formation and development of the wake to downstream is shown in Figure 9a-9d. If splitter distance from SR is increased, formation and size of the wake is changed. By increasing splitter distance from the rear face of SR the wake size increases and average heat transfer is enhanced by about 8 % if taken over the whole effected area of the flat plate, Figure 10.

Splitter distance from the square rod has no effect on the wake position. However, wake size increases by moving the splitter away from the SR and two small wakes are generated on the sides of the splitter. Interaction between the lower wake with the jet flow affects heat transfer, Figure 11 and 12.

If location of the splitter is changed in a vertical direction, Figure 14, although the position of the near wall wake does not change appreciably by this throughout the action, the size of the wake reduces by moving the splitter upwards. Instead two new small wakes form on two sides of the splitter and create a greater effect than seen in previous tests on heat transfer coefficient. The effect appears on the places nearer to the SR and increases the average

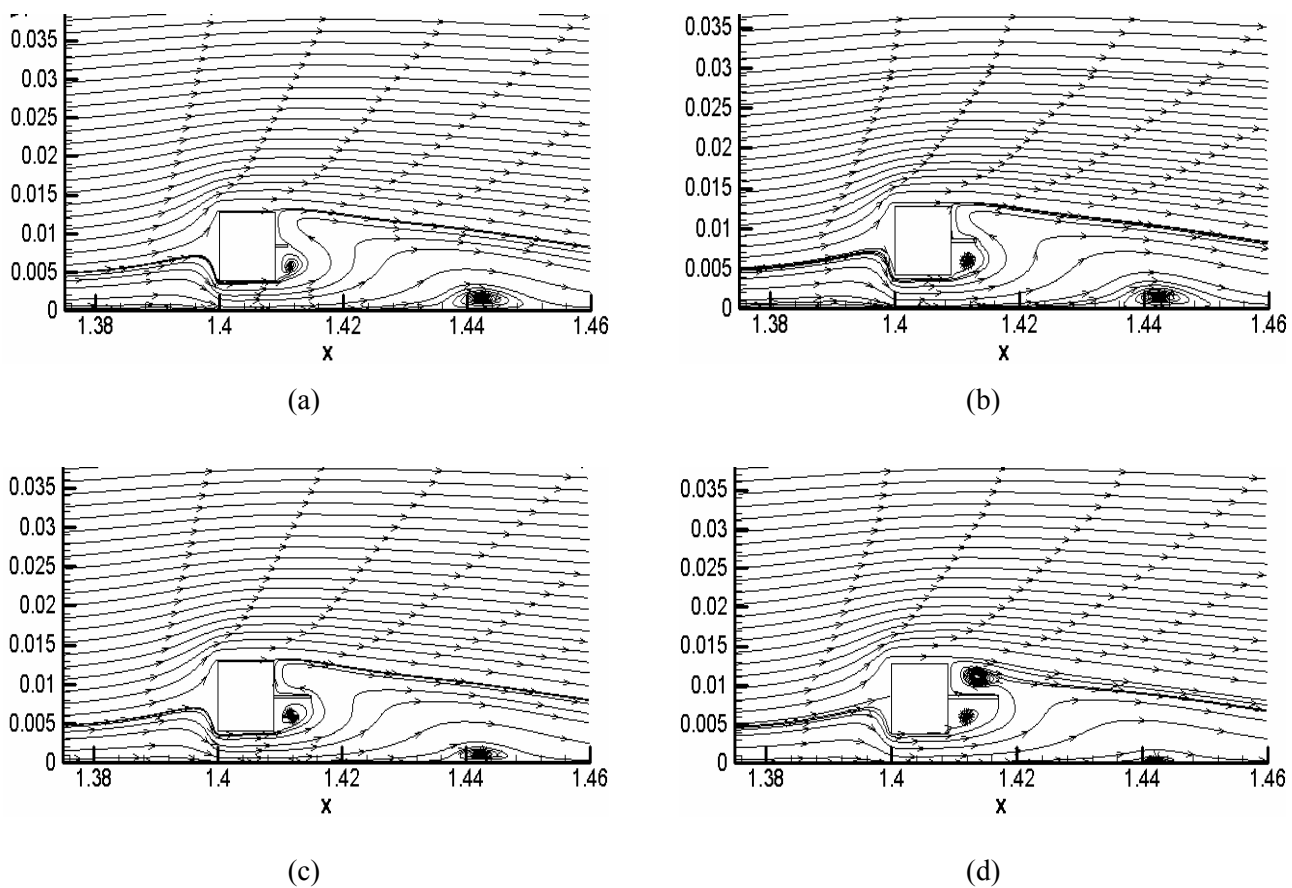


Figure 9. Effect of splitter at rear face of a square rod. Splitter length is changed. Position of SR in the boundary layer and position of splitter are fixed.

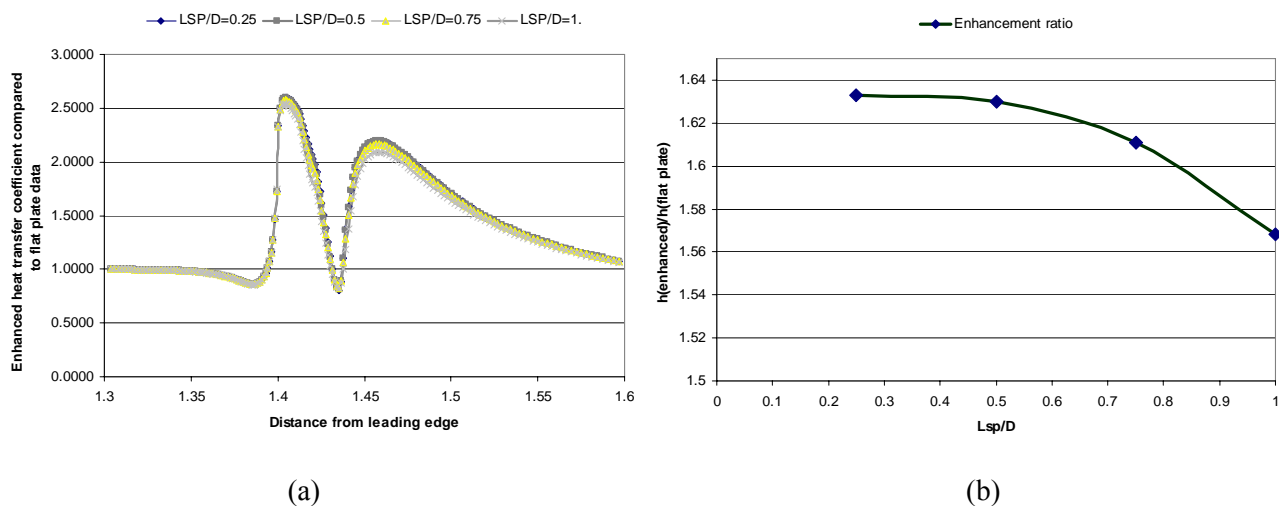


Figure 10. Effect of splitter length on heat transfer coefficient: (a) variation of local heat transfer over flat plate, (b) average heat transfer over $x = 1.3$ to 1.67 , for variation of splitter length.

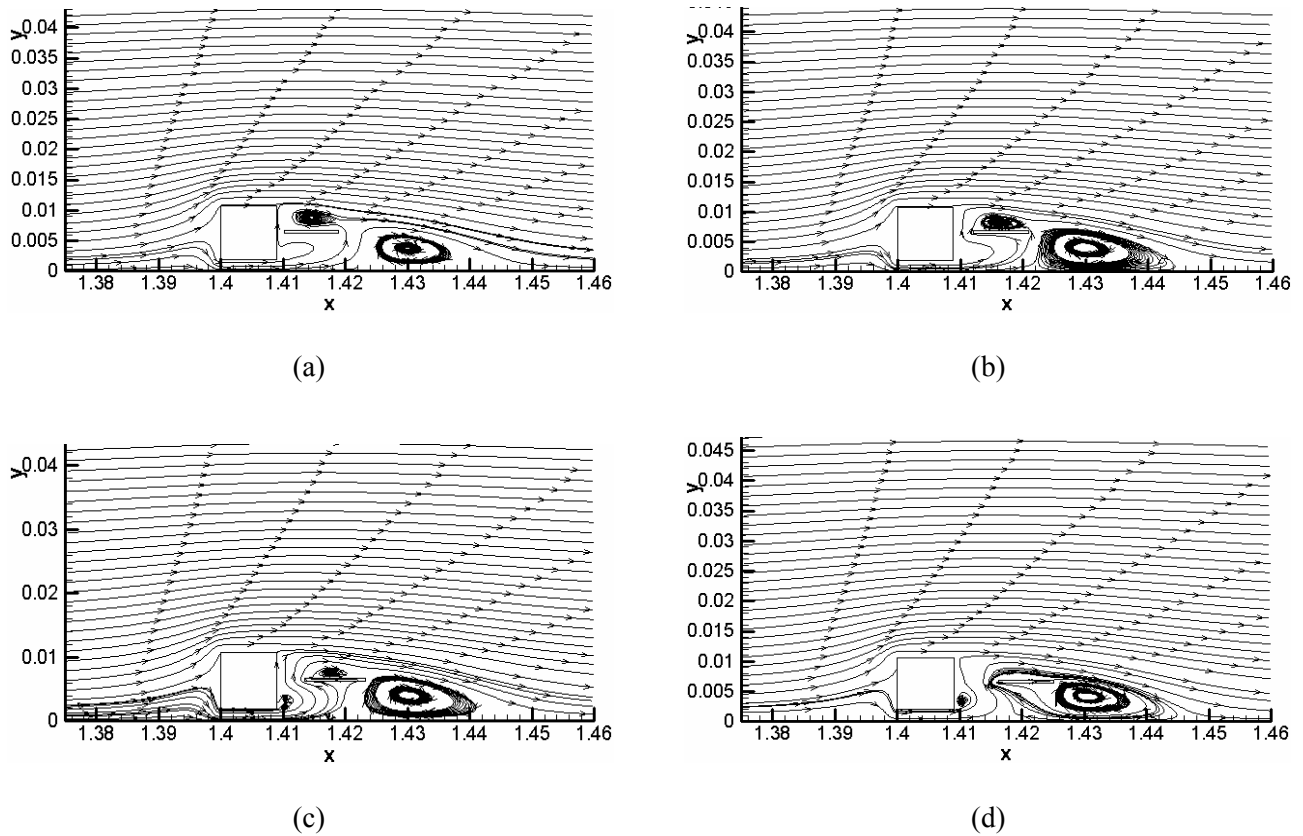


Figure 11. Splitter is placed at variety of distances from rear face of square rod.

overall heat transfer coefficient goes up to 12 %. Figure 13 shows an overall comparison between the effect of square rod distances from a flat plate with a splitter and that of a single square rod. As a general trend, when $H_{sq}/D = 1$ we have maximum heat transfer enhancement. By reducing or increasing distance from the wall, heat transfer decreases. However, splitter distance from the rod is a cause of increasing heat transfer from the flat plate.

4. CONCLUSION

A numerical investigation is made to find how a square rod and splitter downstream to the rear side of SR may affect local and average heat transfer from a flat plate. Results show that a square rod significantly changes the structure of turbulent boundary layer and provokes local heat transfer on

the neighboring flat plate. Local heat transfer increases by a factor of 3 in some locations while on average the increase is up to 60 % over the length of $L_{\text{effected area}} = 28D$ downstream to the SR.

Splitters, in general, directly affect the resulting wake and cause reduced heat transfer from the flat plate. Increase in splitter length decreases average $\overline{h_c}$. If the splitter is displaced parallel to the flat plate down to downstream, $\overline{h_c}$ increases. In another test the splitter is moved away from the wall but attached to the square rod. The effect was to change near wall wake in size and generate new wakes on both sides of the splitter. As a result, average heat transfer increases, Table 1.

It is concluded that if a square rod is positioned inside a turbulent boundary layer it causes increased heat transfer from the wall. In all cases, a splitter if added downstream to the rod, causes reduction of heat transfer from the wall. The

amount of reduction depends on splitter length and its location.

G	Distance between splitter and square rod
H_{sq}	Distance between square rod and flat plate
H_{sp}	Distance between splitter and flat plate
L_{sp}	Splitter length
q	A quantity

5. NOMENCLATURE

D Square rod size

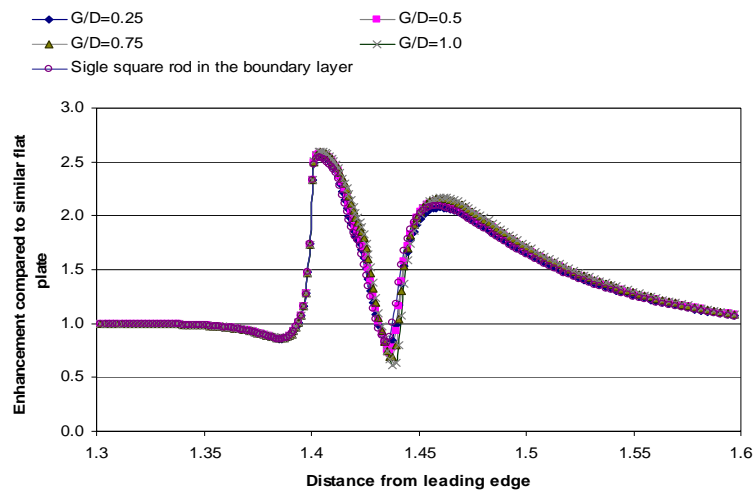


Figure 12. Variation of local heat transfer coefficient affected by splitter distance from rear face of the square rod. An increase of G/D increases average heat transfer coefficient in the effected area. However the splitter reduces average heat transfer coefficient over the flat plate if compared to that of a single rod.

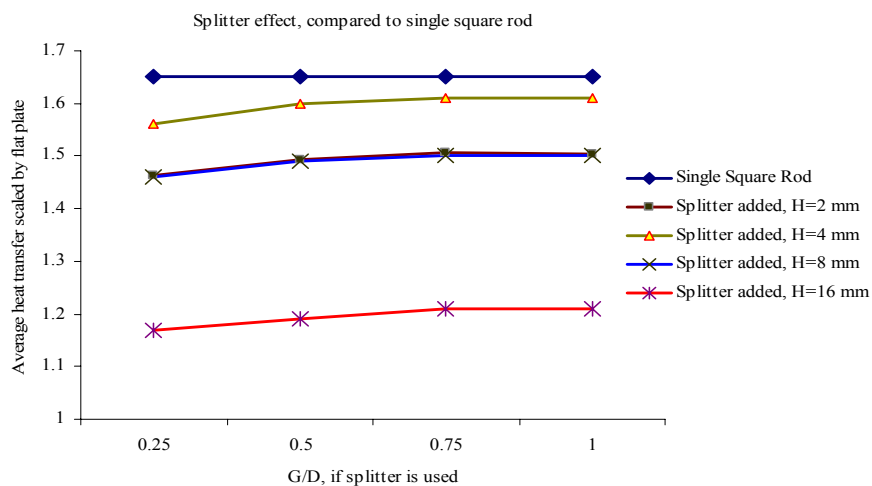
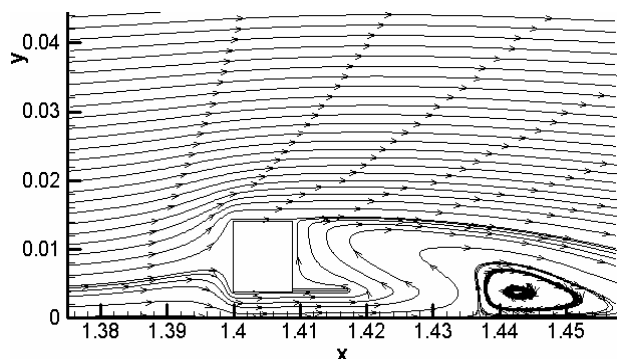


Figure 13. A comparison between results of a single square rod (Farahbod's result), with the effect of square rod with splitter.

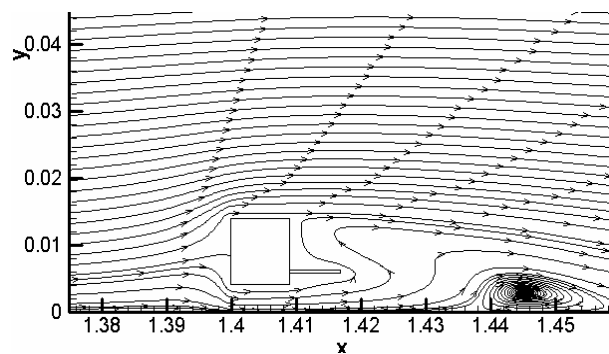
S	Stretching ratio
SR	Square rod
u, v	Velocity components
T	Transpose of a matrix
TEACH	A computer code
x	Distance from flat plate leading edge Zero Pressure Gradients
u^+	u/u_τ , $u_\tau = \sqrt{\tau_w/\rho}$
y^+	$y u_\tau/\nu$
T^+	T/T_τ , $(T_w - T)\rho c u_\tau/q_w$
k^+	k/u_τ^2
ε^+	$\varepsilon \nu/u_\tau^4$
ν_t	Kinematic eddy viscosity
δ	Boundary layer thickness
θ	Temperature difference

6. REFERENCES

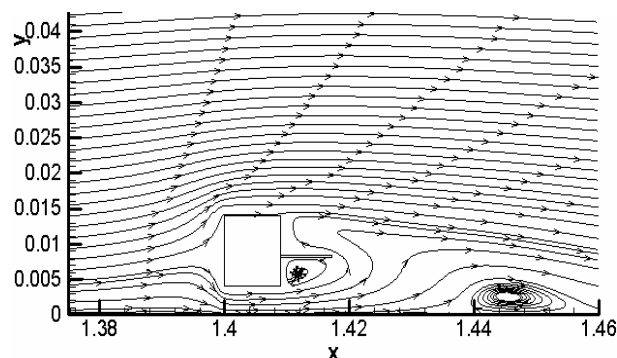
1. Nakayama, A. and Noda, H., "LES Simulation of Flow Around a Bluff Body Fitted with a Splitter Plate", *Journal of Wind Engineering and Industrial Aerodynamics*, (2000), 85-96.
2. Tiwari, S., Chakraborty, D., Biswas, G. and Panigrahi, P. K., "Numerical Prediction of Flow and Heat Transfer in a Channel in The Presence of a Built - in Circular Tube with and Without an Integral Wake Splitter", *International Journal of Heat and Mass Transfer*, (2005), 439-453.
3. Hwang, Jong - Yeon. and Yang, Kyung - Soo., "Reduction of Flow - Induced Forces on a Circular Cylinder Using a Detached Splitter Plate", Department of Mechanical Engineering, Inha University Incheon, Korea, (2000), 402-751.
4. Nathalie Boisaubert, Alain Texier, "Effect of a splitter plate on the near-wake development of a semi - circular cylinder", *Experimental Thermal and Fluid Science*, (1998), 100-111.
5. Anderson, E. A. and Szweczyk, A. A., "Effects of a



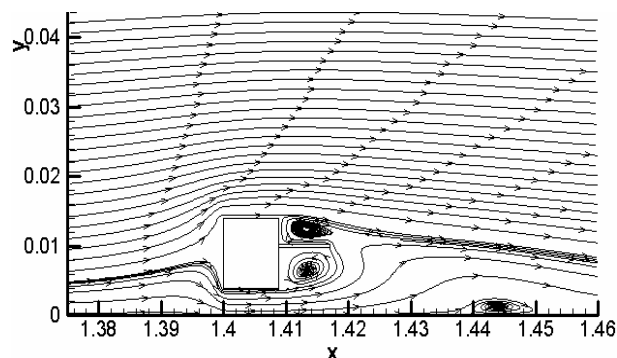
(a)



(b)



(c)



(d)

Figure 14. Position of splitter is changed along vertical direction.

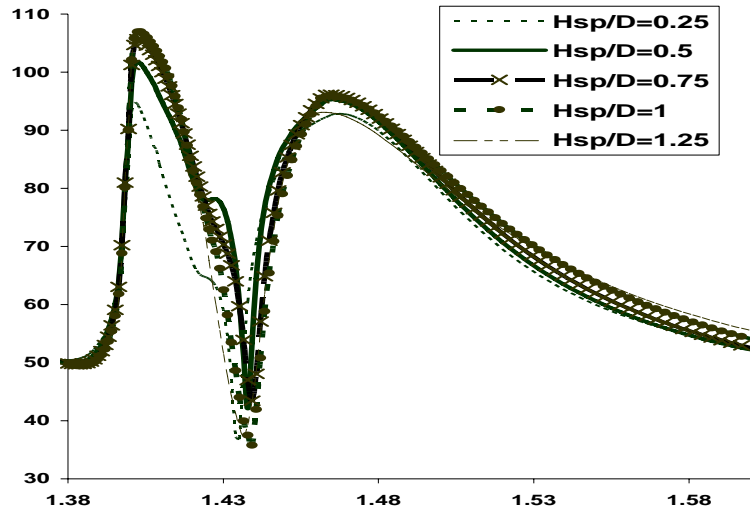


Figure 15. Effect of vertical displacement of splitter on local heat transfer coefficient.

TABLE 1. Average Heat Transfer Enhancement Due to Displacement of Splitter Vertically on the Rear Face of SR.

H_{sp}	$h_c \text{ Average} / h_c \text{ single square rod}$
0.25	1.5
0.5	1.58
0.75	1.6
1.0	1.61

splitter plate on the near wake of a circular cylinder in 2 and 3 - dimensional flow configurations”, *Exp. Fluids*, (1997), 161–174.

6. Farahbode, A. and Kahrom, M., “Heat Transfer Enhancement by Insertion of a Square Rod into a Turbulent Boundary Layer, M.Sc. Thesis, (2004).
7. Gete, Z. and Evans, R. L., “An experimental investigation of unsteady turbulent wake - boundary layer interaction”, *J. of Fluids and Structures*, (2003), 43-45.
8. Xu, G. and Zhou, Y., “Momentum and heat transfer in a turbulent cylinder wake behind a streamwise oscillating cylinder”, *International journal of Heat and Mass Transfer*, (2005), 4062-4072.
9. Kim, J., “Investigation of a Reattachment Turbulent Shear Layer, Flow Over a Backward - Facing Step”,

Tran Sactin of the ASME, *Journal of Fluid Engineering*, (1980), 302-308.

10. Davidson, L., “An Introduction to Turbulence Models”, Publication 97/2, Chalmers University of Technology, Goteborg, Sweden, (2003).
11. Orlanski, I., “A simple Boundary Condition for Unbounded Hyperbolic Flows”, *J. Computational Physics*, Vol. 21, (1976), 251-269.
12. Gresho, P. M., “Seventh Int. Conference Gresho, P. M., Seventh Int. Conf. On Num. Meth. In Laminar and Turbulent Flows”, Stanford Univ., Paloalto, Ca, July, (1991), 15-19.
13. Yang, Y., “Numerical Study of a Backward – Facing Step With Uniform Normal Mass Bleed”, *Int .J. Heat and Mass Transfer*, Vol. 40 , No. 7, Copyright, (1997), 1677–1686.